

# Period-Doubling Route to Chaos in the Hydrogen Peroxide–Sulfur(IV)–Hydrogen Carbonate Flow System<sup>1</sup>

Gyula Rábai

*Institute of Physical Chemistry, Kossuth Lajos University, H-4010 Debrecen, Hungary*

*Received: March 18, 1997; In Final Form: July 1, 1997*<sup>⊗</sup>

Both simulations and experimental results show that a period-doubling route leads from simple pH oscillations through period 2 and period 4 cascades to chaos in an aqueous H<sub>2</sub>O<sub>2</sub>–sulfur(IV)–HCO<sub>3</sub><sup>−</sup> flow system by varying either the removal rate of CO<sub>2</sub> from the reaction mixture or the flow rate. Windows of stable period 3 oscillations are also found in the wide chaotic region calculated in the [H<sub>2</sub>O<sub>2</sub>]<sub>0</sub>–[SO<sub>3</sub><sup>2−</sup>]<sub>0</sub> plane. An autocatalytic production of H<sup>+</sup> during the oxidation of sulfur(IV) by H<sub>2</sub>O<sub>2</sub> is responsible for the positive feedback, while a H<sup>+</sup> consuming negative feedback is provided by the relatively slow reversible formation of CO<sub>2</sub> (HCO<sub>3</sub><sup>−</sup> + H<sup>+</sup> ⇌ CO<sub>2</sub> + H<sub>2</sub>O) and its controlled escape from the surface of the reaction mixture. Protonation of SO<sub>3</sub><sup>2−</sup> also contributes to the removal of the free H<sup>+</sup>. Such a multichannel negative feedback appears to be the clue to the chaotic dynamical behavior. This seems to be the simplest known chaotic chemical reaction system.

## Introduction

Chaos arises from the nonlinear intrinsic nature of deterministic systems. A small number of homogeneous chemical reactions are known to exhibit such a dynamical behavior under favorable conditions.<sup>1–5</sup> All of these reactions have been discovered by chance or by systematic experimental search. An experimentalist should keep in mind that any experimental system is always subject to unavoidable external perturbations that may bring about random responses in a sensitive system. For this reason, a careful analysis of the measured chaotic data is generally recommended to distinguish between such a randomness and chaos of deterministic origin. Finding a route from simple oscillations through more and more complex periodic behavior to chaos with varying a carefully selected bifurcation parameter is even more important for a positive identification of the deterministic origin.

Numerical studies on models with chaotic solutions may reveal additional information unaccessible experimentally. In addition, a good model provides guidelines on how to synthesize chaotic systems using appropriate simple composite reactions as building blocks. We believe that such a synthesis not only would increase the number of chaotic systems but also would be a decisive step toward understanding chemical chaos in a simple way. For this purpose, empirical models composed of measured kinetics equations of composite reactions<sup>6</sup> are favored because they are expected to predict the dynamical behavior of a complex system more reliably than any mechanistic scheme with hypothetical steps and estimated or fitted constant values. We recently found that a simple set of differential equations based on the empirical rate laws of the composite reactions in the H<sub>2</sub>O<sub>2</sub>–sulfur(IV) (S(IV))–marble flow system had a chaotic solution under certain initial conditions. Chaotic oscillations in [H<sup>+</sup>] were also found in the experiments that were designed on the basis of the predictions by the model.<sup>1</sup> That work may be regarded as the first laboratory synthesis of a chaotic chemical system using simple inorganic reactions as building blocks. However, a very high sensitivity of the rate of material transfer on the marble–liquid surface to the external conditions and an ever-changing reactivity of the marble chips during long

experiments appeared to be serious drawbacks in the experimental study. A clear route to chaos from limit cycle oscillations could not be identified. We performed additional numerical simulations with the model to see whether these difficulties can be overcome. The role of the HCO<sub>3</sub><sup>−</sup>/CO<sub>2</sub> couple, which had entered the solution from the marble, turned out to be essential in generating the complex kinetics, but it was not necessary to produce HCO<sub>3</sub><sup>−</sup> in situ. An input flow of its diluted solution was satisfactory. These numerical results suggested that the marble could be replaced by an input solution of NaHCO<sub>3</sub> and K<sub>4</sub>Fe(CN)<sub>6</sub> to obtain a homogeneous chaotic system.<sup>7</sup> Here, instead of the marble, the ferrocyanide–hydrogen peroxide reaction served as a sink for the hydrogen ion. The resulted system appeared to be simpler experimentally than its marble-containing counterpart, but its chemistry became more complex because of the very complex ferrocyanide–hydrogen peroxide reaction.<sup>8</sup> The complex chemistry prevented us from clarifying the mechanism. However, further simulation revealed that the removal of H<sup>+</sup> by the marble or ferrocyanide was not a necessary precondition of the complex dynamics either. It turned out that the HCO<sub>3</sub><sup>−</sup>/CO<sub>2</sub> couple alone can provide a sufficiently strong negative feedback with the necessary time delay for the autocatalytic H<sub>2</sub>O<sub>2</sub>/HSO<sub>3</sub><sup>−</sup> reaction to produce both simple and chaotic oscillations (Table 1). This new finding allows us to leave out the complicated chemistry of the ferrocyanide ion and to construct an even simpler homogeneous system, which makes it possible to perform more convenient and reliable experiments on a chaotic system. Experimental study and simulations of the dynamical behavior in the chaotic H<sub>2</sub>O<sub>2</sub>–S(IV)–HCO<sub>3</sub><sup>−</sup> flow system are reported in this paper. Period-doubling routes to chaos have been disclosed both experimentally and in the simulations.

## Experimental Section

**Materials.** Reagent grade H<sub>2</sub>O<sub>2</sub>, H<sub>2</sub>SO<sub>4</sub>, Na<sub>2</sub>SO<sub>3</sub>, and NaHCO<sub>3</sub> (all Katayama) were used without further purification. Two input solutions were prepared daily: (a) 0.0180 M H<sub>2</sub>O<sub>2</sub>; (b) 0.010 M Na<sub>2</sub>SO<sub>3</sub>, 8.0 × 10<sup>−4</sup> M NaHCO<sub>3</sub>, 3.5 × 10<sup>−4</sup> M H<sub>2</sub>SO<sub>4</sub>. Since it was essential to avoid autoxidation of S(IV) in the reservoir, solution b was kept under N<sub>2</sub> but not bubbled to avoid the loss of the volatile components. Had solution b in

<sup>⊗</sup> Abstract published in *Advance ACS Abstracts*, August 15, 1997.

**TABLE 1: Component Reactions and Empirical Rate Laws of the Chaotic H<sub>2</sub>O<sub>2</sub>–S(IV)–HCO<sub>3</sub><sup>–</sup> System**

no.	reactions	rate laws
(1)	H <sub>2</sub> O <sub>2</sub> + HSO <sub>3</sub> <sup>–</sup> → H <sup>+</sup> + SO <sub>4</sub> <sup>2–</sup> + H <sub>2</sub> O	R <sub>1</sub> = (k <sub>1</sub> + k <sub>1</sub> '[H <sup>+</sup> ])[HSO <sub>3</sub> <sup>–</sup> ][H <sub>2</sub> O <sub>2</sub> ]
(2)	HSO <sub>3</sub> <sup>–</sup> ⇌ H <sup>+</sup> + SO <sub>3</sub> <sup>2–</sup>	R <sub>2</sub> = k <sub>2</sub> [HSO <sub>3</sub> <sup>–</sup> ]; R <sub>–2</sub> = k <sub>–2</sub> [H <sup>+</sup> ][SO <sub>3</sub> <sup>2–</sup> ]
(3)	CO <sub>2</sub> (aq) + H <sub>2</sub> O ⇌ H <sup>+</sup> + HCO <sub>3</sub> <sup>–</sup>	R <sub>3</sub> = k <sub>3</sub> [CO <sub>2</sub> (aq)]; R <sub>–3</sub> = k <sub>–3</sub> [H <sup>+</sup> ][HCO <sub>3</sub> <sup>–</sup> ]
(4)	CO <sub>2</sub> (aq) → CO <sub>2</sub> (gas)	R <sub>4</sub> = k <sub>4</sub> [CO <sub>2</sub> (aq)]

the reservoir been bubbled, some loss of CO<sub>2</sub> and SO<sub>2</sub> would have been unavoidable despite the slightly alkaline pH.

**Reactor.** The continuous flow experiments were performed in a glass vessel described earlier.<sup>1</sup> The reactor was covered with a silicon cap in all the experiments, but a hole (i.d. 7.0 mm) was drilled through the cap to ensure a smooth flow of the gas stream out of the reactor. If CO<sub>2</sub> was allowed to accumulate in the air space of the reactor, the oscillatory behavior was only transient and a steady state set in slowly. A pH electrode, the input (i.d. 1.0 mm), and output tubes (i.d. 2.0 mm) were led through the cap. N<sub>2</sub> gas entered the reactor through a Tanaka E.W. controller, a Koflac flow meter, and a capilar (i.d. 0.3 mm).

**Procedure.** Earlier we found<sup>1</sup> that low temperature was more favorable for complex dynamical behavior than room temperature. Thus all our present experiments were carried out at 4.0 °C. The reactor was placed in a thermostated water bath, on a waterproof stirrer motor, and was fed with prethermostated input solutions by means of a peristaltic pump (Eyela 3M) as described earlier.<sup>1</sup> The excess of the liquid was removed with a second pump. The liquid level could be controlled by the vertical position of the outlet tubes. The mixture was continuously stirred with a magnetic stirrer bar at 500 rpm. The pH and the temperature inside the reactor were continuously measured. The experiments were started by filling the reactor with the input solutions at the highest pump speed available (5.0 mL/min). After the reactor had been filled, the pump speed was reduced to the desired value. The volume of liquid in the reactor was 27.0 mL.

**Computation.** A semiimplicit Runge–Kutta method<sup>9</sup> with an error parameter of 10<sup>–5</sup> was used for numerical integrations. This low value of the error parameter was proved to be necessary and sufficient for obtaining correct results. The existence of chaos was identified by calculating period-doubling sequences as we varied an appropriate parameter.

## Results

**Modeling.** Our earlier scheme for the related H<sub>2</sub>O<sub>2</sub>–S(IV)–marble system<sup>1</sup> was preserved with a simplification: The composite reaction describing the dissolution of the marble is not relevant and was left out. The rest of the model and the corresponding rate laws are shown in Table 1. It is striking that the model is very simple and very well supported by the empirical rate laws reported for the composite reactions. The stoichiometry of reaction 1 along with the second term of R<sub>1</sub> reflects that reaction 1 is autocatalytic in H<sup>+</sup>. The rate laws of reactions 2–4 have the simplest possible forms. Kinetics of the composite reactions have been studied separately, and the measured rate constant values are available<sup>1</sup> (Table 2). It is important that both the hydration of CO<sub>2</sub> (reaction 3) and the consumption of H<sup>+</sup> in the reverse reaction –3 are slow<sup>10, 11</sup> in the pH range of interest. The reason of this unique slowness is that just a small fraction of HCO<sub>3</sub><sup>–</sup> can be protonated in a fast reaction if pH > 5, because H<sub>2</sub>CO<sub>3</sub> is a relatively strong acid

**TABLE 2: Rate Constants Used in the Calculations<sup>a</sup>**

	25.0 °C	4.0 °C	ref
k <sub>1</sub> M <sup>–1</sup> s <sup>–1</sup>	7.0	1.5	1, 14
k <sub>1</sub> ' M <sup>–2</sup> s <sup>–1</sup>	1.48 × 10 <sup>7</sup>	6.5 × 10 <sup>6</sup>	1, 14
k <sub>2</sub> s <sup>–1</sup>	3.0 × 10 <sup>3</sup>	1.0 × 10 <sup>3</sup>	1, 14
k <sub>–2</sub> M <sup>–1</sup> s <sup>–1</sup>	5.0 × 10 <sup>10</sup>	1.0 × 10 <sup>10</sup>	1, 14
k <sub>3</sub> s <sup>–1</sup>	4.3 × 10 <sup>–2</sup>	1.1 × 10 <sup>–2</sup>	1, 10
k <sub>–3</sub> M <sup>–1</sup> s <sup>–1</sup>	9.6 × 10 <sup>4</sup>	2.5 × 10 <sup>4</sup>	1
k <sub>4</sub> s <sup>–1</sup>		(1.5–5.0) × 10 <sup>–3</sup>	

<sup>a</sup> Apparent activation energies for the rate constants were used with values available at 25.0 °C to calculate values for 4.0 °C.

**TABLE 3: Differential Equations with Chaotic Solutions in the H<sub>2</sub>O<sub>2</sub>–S(IV)–HCO<sub>3</sub><sup>–</sup> Flow System<sup>a</sup>**

$$\begin{aligned} d[\text{SO}_3^{2-}]/dt &= R_2 - R_{-2} + k_0([\text{SO}_3^{2-}]_0 - [\text{SO}_3^{2-}]) \\ d[\text{H}_2\text{O}_2]/dt &= -R_1 + k_0([\text{H}_2\text{O}_2]_0 - [\text{H}_2\text{O}_2]) \\ d[\text{HSO}_3^-]/dt &= -R_1 - R_2 + R_{-2} - k_0[\text{HSO}_3^-] \\ d[\text{H}^+]/dt &= R_1 + R_2 - R_{-2} + R_3 - R_{-3} + k_0([\text{H}^+]_0 - [\text{H}^+]) \\ d[\text{HCO}_3^-]/dt &= R_3 - R_{-3} + k_0([\text{HCO}_3^-]_0 - [\text{HCO}_3^-]) \\ d[\text{CO}_2(\text{aq})]/dt &= -R_3 + R_{-3} - R_4 - k_0[\text{CO}_2(\text{aq})] \end{aligned}$$

<sup>a</sup> The inverse residence time of the CSTR (termed flow rate in the text) is k<sub>0</sub> in units of s<sup>–1</sup>. The input concentrations in the feed (indicated with 0 in the subscript) and the actual concentrations in the reactor (no subscript) are given in M.

(K<sub>d</sub> = 2.5 × 10<sup>–4</sup> M at 25 °C). However, H<sub>2</sub>CO<sub>3</sub> decomposes to CO<sub>2</sub> and H<sub>2</sub>O in a slow reaction that shifts the protonation equilibrium and makes it possible for most of the HCO<sub>3</sub><sup>–</sup> to be protonated in a slow reaction even at pH > 5. Due to the slowness of the decomposition of H<sub>2</sub>CO<sub>3</sub>, the overall rate of the H<sup>+</sup> removal is determined by this slow decomposition.



Consequently the autocatalytic generation of H<sup>+</sup> can be completed before significant removal of H<sup>+</sup> takes place (time delay between the positive and the negative feedbacks). If reaction 3 were a fast equilibrium, it would act as an acid base buffer and would prevent any pH oscillation in the system. Summarized in Table 3 are the differential equations of the variable species with flow terms. Numerical solution of the differential equation system indicated the existence of chaotic regimes and disclosed that changing either the flow rate of the liquid input (k<sub>0</sub>) or the rate of the selective removal of CO<sub>2</sub> (k<sub>4</sub>) caused the system to undergo a transition from simple regular oscillations through a period-doubling route to chaos at fixed input species concentrations. Figure 1 shows the evolution of the calculated pH time series from simple low-frequency oscillations (panel A, top) through period 2 and period 4 (2 and 4 peaks in each period, respectively) to chaos (bottom on panel A) at fixed k<sub>0</sub> with decreasing k<sub>4</sub> as a bifurcation parameter. Upon further decrease in k<sub>4</sub> value, chaos is replaced by period 3 oscillations (panel B, top), indicating that a periodic window exists in the chaotic regime. Such windows are a universal feature of the period-doubling route to chaos.<sup>12</sup> At even smaller k<sub>4</sub>, another type of chaos can be calculated that undergoes a reverse period-doubling route with further decreasing k<sub>4</sub> leading to high-frequency simple oscillations at k<sub>4</sub> = 1.50 × 10<sup>–3</sup> s<sup>–1</sup>. These calculations predict that low-frequency simple oscillations are expected in the experiments when CO<sub>2</sub> is removed from the reaction mixture at a high rate and high-frequency regular oscillations may exist when the escape of CO<sub>2</sub> is slow. Apparently, the chaotic behavior results in between from the interaction of the two regular oscillations characterized with different frequencies. Similar series can be calculated with varying k<sub>0</sub> from 9.0 × 10<sup>–4</sup> (low frequency), through 8.0 × 10<sup>–4</sup> (period 2), 7.0 × 10<sup>–4</sup> (period 4), (3.5–6.5) × 10<sup>–4</sup> (chaos,

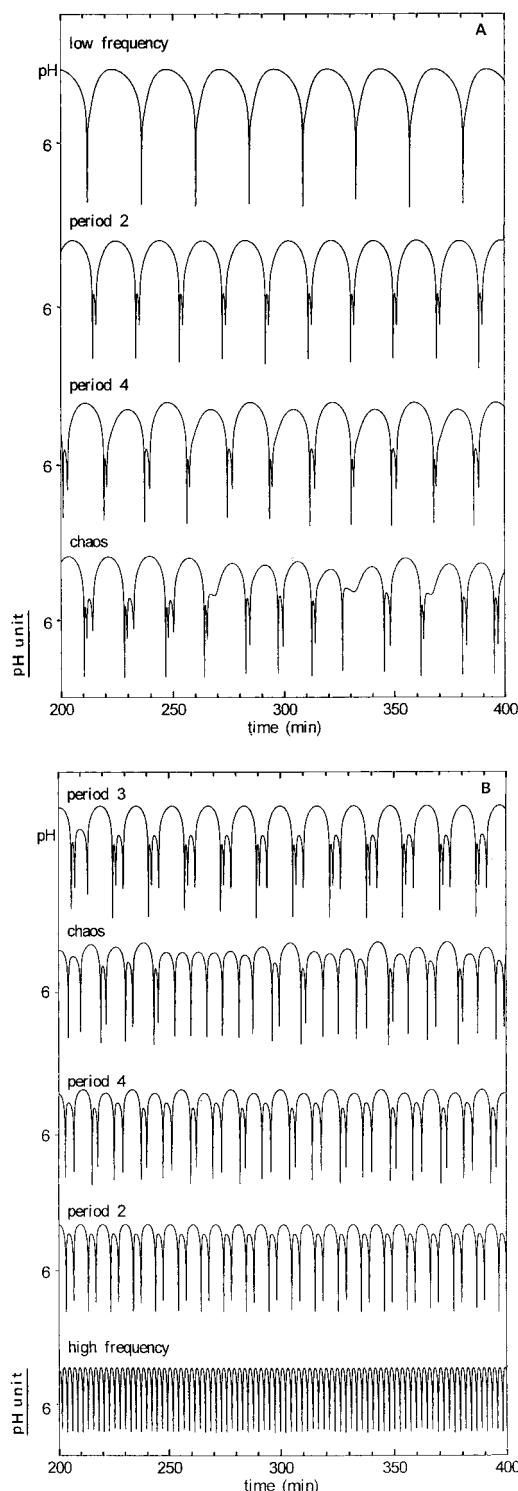


**Figure 1.** Calculated pH–time responses at different rates of CO<sub>2</sub> escape.  $k_4 \times 10^3 \text{ s}^{-1}$ : from the top in panel A, 5.0, 3.4, 3.1, 2.6; from the top in panel B, 2.3, 2.2, 2.1, 2.0, 1.5, respectively. Rate constants given in Table 2 for 4.0 °C,  $k_0 = 3.0 \times 10^{-4} \text{ s}^{-1}$ ,  $[\text{H}_2\text{O}_2]_0 = 0.013$ ,  $[\text{SO}_3^{2-}]_0 = 5.0 \times 10^{-3}$ ,  $[\text{H}^+]_0 = 3.9 \times 10^{-4}$ , and  $[\text{HCO}_3^-]_0 = 4.0 \times 10^{-4} \text{ M}$  were used in the calculations.

unusually large interval),  $3.3 \times 10^{-4}$  (period 3),  $(2.7\text{--}3.0) \times 10^{-4}$  (chaos),  $2.5 \times 10^{-4}$  (period 4),  $2.2 \times 10^{-4}$  (period 2) to  $1.8 \times 10^{-4} \text{ s}^{-1}$  (high frequency) at fixed  $k_4 = 2.2 \times 10^{-3} \text{ s}^{-1}$  and at constant input concentrations shown in Figure 1. Calculations indicate that the input concentration values of H<sup>+</sup> and HCO<sub>3</sub><sup>−</sup> should be chosen close to each other with a small excess of HCO<sub>3</sub><sup>−</sup> in order for the model to produce such a complex behavior. The calculated behavior is more sensitive to the change in removal rate of CO<sub>2</sub> than to  $k_0$ .

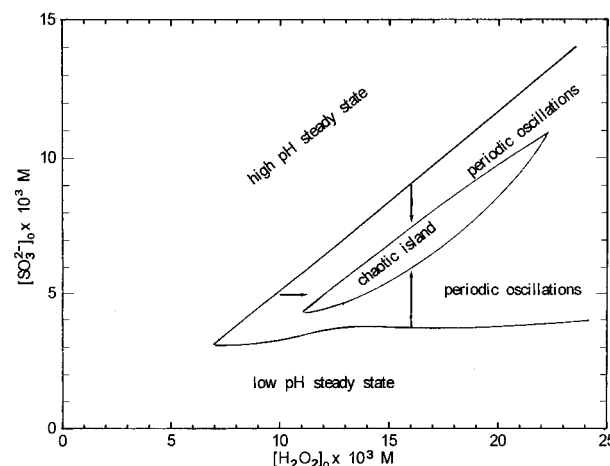


**Figure 2.** Calculated two-parameter bifurcation diagram in the  $[\text{H}_2\text{O}_2]_0$ – $[\text{SO}_3^{2-}]_0$  plane. Fixed parameters: rate constants are given in Table 2 for 4.0 °C,  $k_4 = 2.2 \times 10^{-3} \text{ s}^{-1}$ ,  $k_0 = 3.0 \times 10^{-4} \text{ s}^{-1}$ ,  $[\text{H}^+]_0 = 3.9 \times 10^{-4}$ , and  $[\text{HCO}_3^-]_0 = 4.0 \times 10^{-4} \text{ M}$ . The arrows indicate period-doubling routes. The island of chaotic region contains periodic islets (not shown).

A calculated two-parameter bifurcation diagram in the  $[\text{SO}_3^{2-}]_0$ – $[\text{H}_2\text{O}_2]_0$  plane is shown in Figure 2. Regions of steady states and periodic and chaotic oscillations are separated with solid lines. The simplest period 1 oscillations could be calculated close to the line separating the steady state and periodic regions. Moving off this line inside the oscillatory region toward the island of chaos, more and more complex periodic behavior results. The island of the chaos is surrounded by regions of complex periodic oscillations. The arrows indicate some possible ways for period-doubling routes from simple oscillations through period 2 and period 4 cascades to chaos. Most of the territory of the island marked “chaotic region” represents true chemical chaos, but there are small islets of periodic oscillations (mostly period 3) in this region as well. These periodic islets are not indicated in Figure 2. One should keep in mind that choosing concentrations in a chaotic region thus does not guarantee that chaotic behavior will exclusively result.

The reaction is a true continuously stirred tank reactor (CSTR) oscillator because all six variables oscillate. We note that the number of variables can be reduced to four without losing the chaotic character of the model because  $[\text{H}_2\text{O}_2]$  can be treated as constant and there is a stoichiometric connection between  $\text{SO}_3^{2-}$  and  $\text{HSO}_3^-$ . However, we do not favor any further simplification because the behavior of the simplified model becomes less similar to the behavior of the real system.

**Experimental Results.** Since the model is closely related to the real chemistry and it does not contain any hypothetical steps or roughly estimated constant values, one may well expect that the calculated pH time series can be realized experimentally under the predicted conditions. Indeed, we have found most of the predicted curves in our experiments. The experimental conditions were almost identical to those used in the numerical simulations. However, we had to apply somewhat different input concentrations for H<sub>2</sub>O<sub>2</sub> and H<sup>+</sup> in the experiments such as  $[\text{H}_2\text{O}_2]_0 = 0.0090 \text{ M}$  (not 0.013 M) and  $[\text{H}^+]_0 = 3.5 \times 10^{-4} \text{ M}$  (not  $3.9 \times 10^{-4} \text{ M}$ ) in order to be able to observe period doublings similar to their calculated counterparts. The necessity of these modifications may be understood because the rate constants of reaction 1 were determined<sup>1</sup> with roughly 20–30% error at 4.0 °C. If the real values are higher than their determined counterparts, using smaller  $[\text{H}_2\text{O}_2]_0$  may compensate this error (see  $R_1$ ). On the other hand, commercial Na<sub>2</sub>SO<sub>3</sub> contains some NaHSO<sub>3</sub>, which provides some extra H<sup>+</sup> after

the oxidation to S(VI), making it necessary to apply smaller  $[H^+]_0$  in the experiments than in the calculations.

Variation of the removal rate of  $CO_2$  was achieved by changing the flow rate of the  $N_2$  stream passing through the CSTR. In this way we could not observe the period-doubling route from low-frequency oscillations to chaos because it was not possible to remove  $CO_2$  from the CSTR as fast as it should have been necessary to support this phenomenon. However, the period-doubling route from high-frequency oscillations to chaos was nicely measurable. At the highest controllable  $N_2$  flow rate, we observed chaotic pH changes (Figure 3A, top). With decreasing  $N_2$  flow rate, stable period 3 oscillations (Figure 3A, middle), another type of chaos (Figure 3A, bottom), period 4, period 2, and high-frequency period 1 oscillations (Figure 3B) could be measured. The amplitudes of the measured curves (2–2.8 pH units) were higher than the calculated ones (1–2 pH units), but other features are strikingly similar. Very similar series were measured while varying the liquid flow rate at fixed  $N_2$  flow rate. Using input concentrations given in Figure 3 and  $20.0 \pm 1.0$  mL/min  $N_2$  flow rate, we measured low-frequency regular oscillations at  $k_0 = 10.1 \times 10^{-4} s^{-1}$ , period 2 at  $k_0 = 8.9 \times 10^{-4} s^{-1}$ . Transient period 4 oscillations at  $k_0 = 8.5 \times 10^{-4} s^{-1}$  were also measurable, but these traces could not be maintained for long time because they became chaotic during a long run. Sustained chaotic curves similar to that shown in Figure 3A (top) were measured in a wide range of  $k_0$  ( $3.7$ – $8.4$ )  $\times 10^{-4} s^{-1}$ . The chaos could be approached from the other direction as well: at  $k_0 = 1.5 \times 10^{-4} s^{-1}$  high-frequency oscillations, at  $k_0 = 2.5 \times 10^{-4} s^{-1}$  period 2, at  $k_0 = 2.7 \times 10^{-4} s^{-1}$  period 4, at  $k_0 = (2.8$ – $3.5) \times 10^{-4} s^{-1}$  chaos, and at  $k_0 = 3.6 \times 10^{-4} s^{-1}$  period 3 oscillations were found. Again the region of chaos is surprisingly large. If the sulfite-containing solution contacted air oxygen, chaotic and periodic behavior in the CSTR was only transient; the system assumed a steady state in a few hours as the sulfite concentration decreased due to autoxidation in the reservoir or to the escape of  $SO_2$ .

Both our simulation calculations and the experiments clearly show that the chaotic behavior is very sensitive to the rate of the escape of  $CO_2$  gas from the reaction mixture to the air (process 4). This composite reaction seems to be essential for sustained chaotic behavior. A few runs in a reactor with no air space indicated that any periodic or chaotic oscillatory behavior can only be transient and steady state can eventually be observed in a long run if the escape of  $CO_2$  from the reactor is prevented. This observation is in good agreement with the results of the simulation calculations.

## Discussion

A combination of the  $H_2O_2$ – $HSO_3^-$  reaction with the  $CO_2$ – $HCO_3^-$  equilibrium results in a chaotic system that is very convenient to study both experimentally and numerically. Its simplicity is especially attractive.  $CO_2$  and  $HCO_3^-$  are probably not subjected to any redox transformation under the conditions, and they are not expected to interfere the  $H_2O_2$ – $HSO_3^-$  reaction. Since the only common intermediate is  $H^+$ , the composite reactions can interact only via the hydrogen ion. Since the mixing should be perfect on the time scale of this oscillator, we do not think that the mixing would, in any way, contribute to the chaotic behavior in the CSTR runs.

The chaos is robust, and its reproducibility is rather good if the experimental parameters are controlled carefully. The best bifurcation parameters appeared to be  $k_0$  and  $k_4$ . The chaos exists in a surprisingly wide range of both  $k_0$  and  $k_4$ . Experimental observation of the period-doubling cascades from low-frequency oscillations to chaos with changing rate of  $CO_2$  escape

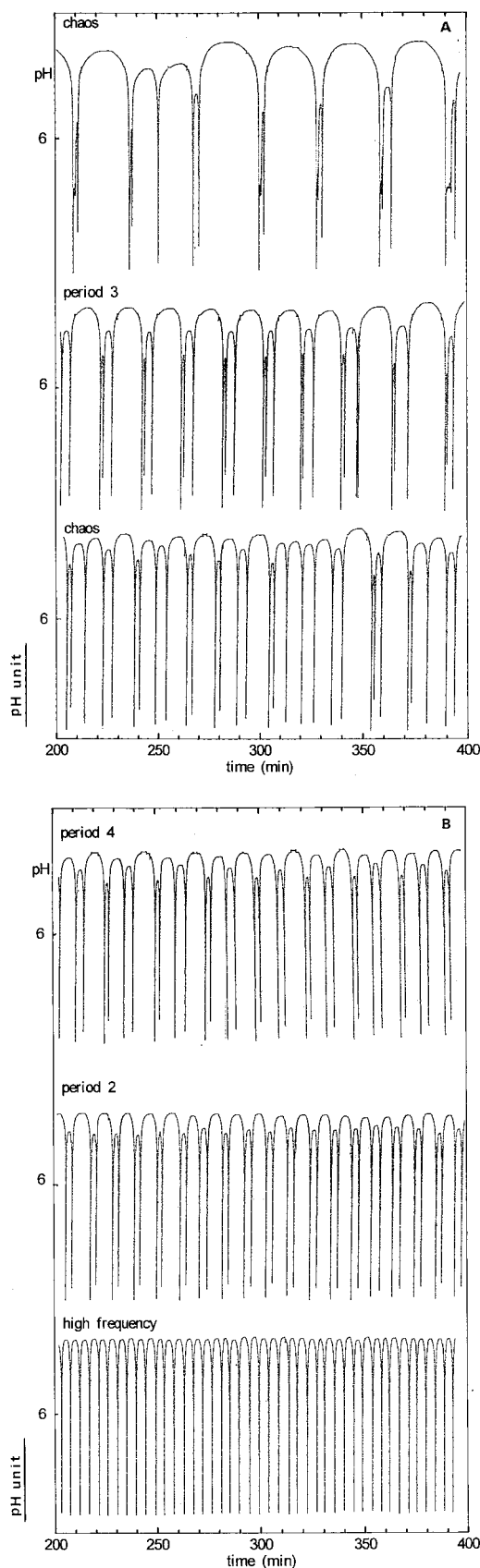


**Figure 3.** Fractions of the main types of the measured pH–time curves at 4.0 °C in a CSTR.  $N_2$  flow rate (mL/min): from the top in panel A,  $61 \pm 5$ ,  $25.0 \pm 1.2$ ,  $20.0 \pm 1.0$ ; from the top in panel B,  $17.0 \pm 0.9$ ,  $15.0 \pm 0.7$ ,  $9.0 \pm 0.5$ , respectively.  $k_0 = 3.0 \times 10^{-4} s^{-1}$ ,  $[H_2O_2]_0 = 0.0090$ ,  $[SO_3^{2-}]_0 = 5.0 \times 10^{-3}$ ,  $[H^+]_0 = 3.5 \times 10^{-4}$ ,  $[HCO_3^-]_0 = 4.0 \times 10^{-4}$  M.

was, however, prevented because the removal rate of  $CO_2$  ( $k_4$ ) cannot be increased at will. With changing  $k_0$ , the period-

doubling route was found from both low- and high-frequency oscillations. One can also find period-doubling routes in the  $\text{H}_2\text{O}_2\text{--SO}_3^{2-}$  plane as one approaches the island of chaotic behavior in the region of periodic oscillations.

The chemical background of this dynamical behavior seems to be clear. Results of separate kinetics studies on the composite reactions are available in the literature and can be used for modeling very successfully. Simulation calculations show that the chaotic behavior is inherent in the differential equations of the system. The model is very simple but nevertheless describes correctly the complex dynamics indicating that  $\text{H}^+$  plays a crucial governing role. A positive feedback is generated by reaction 1, which is autocatalytic in  $\text{H}^+$ , as it is reflected by the second term of rate law  $R_1$ . The necessary negative feedback is provided by the protonation of  $\text{HCO}_3^-$  (reverse reaction 3) as it removes  $\text{H}^+$  in the form of  $\text{CO}_2 + \text{H}_2\text{O}$  when the pH is low. It is crucial that reaction 3 is slow compared to other protonation equilibria.<sup>11</sup> This unique slowness ensures a time delay that separates the proton-consuming pathway from the fastest part of the positive feedback channel in which the proton is produced. Despite of the simplicity of the system, the proton-consuming pathway consists of several channels.  $\text{CO}_2$  can be regarded as a precursor of  $\text{H}^+$  (see reaction 3). A combination of the reverse reaction 3 with a first-order escape of  $\text{CO}_2$  in process 4, and with an additional channel for proton consumption in reverse reaction 2, results in a multichannel negative feedback mechanism. Similarly, in a general model of the chaotic chlorite oscillators,<sup>13</sup> three channels are available for the removal of the autocatalyst ( $\text{HOCl}$ ) or its precursor ( $\text{Cl}_2\text{O}_2$ ). A multichannel negative feedback pathway seems to be a vital element for the chaotic nature of the present system and of some other chaotic chemical reactions.

## Conclusion

In light of the present results, combination of the  $\text{CO}_2/\text{HCO}_3^-$  equilibrium with autocatalytic  $\text{H}^+$ -producing reactions is expected to be a fruitful approach for designing systems with

oscillatory and chaotic dynamics. Such a "synthesis" not only would increase the number of the chaotic systems but also would be a big step forward in understanding their mechanism on the basis of pure chemistry.

It is also noteworthy that the breathing in mammals is brought about by the muscles of diaphragm and intercostal muscles. The rhythmic movements of these muscles are controlled by a respiratory center, which is sensitive to the increased  $\text{CO}_2$  pressure in the lung. The key role of  $\text{CO}_2$  in the control mechanism of respiratory cycles is obvious. It remains to be seen if there is any formal analogy between the role of  $\text{CO}_2$  in the control of respiratory cycles and in the simple inorganic oscillatory systems.

**Acknowledgment.** This work was supported by the Hungarian Science Foundation (OTKA T14440).

## References and Notes

- (1) pH Oscillations with Marble. 3. Part 2: Rábai, Gy.; Hanazaki, I. *J. Phys. Chem.* **1996**, *100*, 15454.
- (2) Olsen, L. F.; Degn, H. *Nature* **1977**, *267*, 177.
- (3) Schmitz, R. A.; Graziani, K. R.; Hudson, J. L. *J. Chem. Phys.* **1977**, *67*, 3040.
- (4) Orbán, M.; Epstein, I. R. *J. Phys. Chem.* **1982**, *86*, 3907.
- (5) Doona, J. C.; Doumbouya, S. I. *J. Phys. Chem.* **1994**, *98*, 513.
- (6) Rábai, Gy.; Bazsa, Gy.; Beck, M. T. *J. Am. Chem. Soc.* **1979**, *101*, 6746.
- (7) Rábai, Gy.; Kaminaga, A.; Hanazaki, I. *J. Chem. Soc., Chem. Commun.* **1996**, 2181.
- (8) Rábai, Gy.; Kustin, K.; Epstein, I. R. *J. Am. Chem. Soc.* **1989**, *111*, 8271.
- (9) Kaps, P.; Rentrop, P. *Numer. Math.* **1979**, *33*, 55.
- (10) Eigen, M.; Kruse, W.; Maass, G.; De Maeyer, L. in *Progress in Reaction Kinetics*; Porter, G., Ed.; Pergamon Press: New York, 1964; Vol. 2, p 285.
- (11) Degn, H.; Kristensen, B. *J. Biochem. Biophys. Methods* **1986**, *12*, 305.
- (12) Steinmetz, C. G.; Geest, T.; Larter, R. *J. Phys. Chem.* **1993**, *97*, 5649.
- (13) Rábai, Gy.; Orbán, M. *J. Phys. Chem.* **1993**, *97*, 5935.
- (14) Rábai, Gy.; Kustin, K.; Epstein, I. R. *J. Am. Chem. Soc.* **1989**, *111*, 3870.